FACTA UNIVERSITATIS
Series: **Electronics and Energetics** Vol. 35, Nº 3, September 2022, pp. 455-468
https://doi.org/10.2298/FUEE2203455N

Original scientific paper

EXPERIMENTAL SHIELDING EFFECTIVENESS STUDY OF METAL ENCLOSURE WITH ELECTROMAGNETIC ABSORBER INSIDE

Nataša Nešić[1], Nebojša Dončov[2], Slavko Rupčić[3], Vanja Mandrić-Radivojević[3]

[1]Department of Information and Communication Technologies, Academy of Applied Technical and Preschool Studies, Niš, Serbia
[2]Faculty of Electronic Engineering, University of Niš, Serbia
[3]Faculty of Electrical Engineering, University of Josip Juraj Strossmayer, Osijek, Croatia

Abstract. *In this paper, the impact of an electromagnetic absorber inside a protective metal enclosure is analyzed. The absorber is put inside the enclosure in order to improve its shielding effectiveness, especially at the first resonant frequency. Different absorber's sheet positions inside the enclosure are analyzed. The absorber sheet dimensions are fitted to correspond the enclosure's walls. The experimental procedure is conducted in a semi-anechoic room. The numerical TLM simulations of the EM filed distribution inside enclosure are conducted in order to consider position of the absorber sheet on different walls.*

Key words: *Absorber, Enclosure, EMI absorber sheet, Measurements, Shielding Effectiveness, TLM method.*

1. INTRODUCTION

An increasing number of modern electronic devices resulted in the rise of electromagnetic (EM) radiation. Hence, it is of considerable importance to conduct electromagnetic compatibility (EMC) analysis. Quantifying the shielding properties of an enclosure can be considered from the viewpoint of shielding effectiveness (SE).

Commonly, a shielding characteristic of an enclosure can be given as a ratio of EM fields with and without an enclosure at some probe point, over a wide frequency range. The SE of enclosure may be very low or even has negative value at the resonant frequencies in the observed frequency range. The negative values of the enclosure SE at the resonant

Received March 1, 2022; revised March 24, 2022; accepted May 15, 2022
Corresponding author: Nataša Nešić
Department of Information and Communication Technologies, Academy of Applied Technical and Preschool Studies, Aleksandra Medvedeva 20, 18000 Niš, Serbia
E-mail: natasa.nesic@akademijanis.edu.rs
*An earlier version of this paper was presented at the 15th International Conference on Applied Electromagnetics - ΠΕС 2021, August 30th - September 1st, 2021, in Niš, Serbia [1].

frequencies can affect or even can compromise the useful frequency range, in which EM shielding of a device is provided.

A number of different methods such as the analytical, the numerical and the experimental ones can be used, in order to study the shielding characteristic of an enclosure. The analytical methods [2]–[4] are usually based on problem simplification, thus they can be very fast but with some inherent limitations. For an efficient computational modelling of protective enclosures, there are numerous numerical techniques. One among many is the Transmission-Line Matrix (TLM) method [5], which will be employed in this paper. Finally, in the experimental methods, an antenna is set inside the enclosure in order to measure its SE. Furthermore, the physical dimensions of an in-house monopole receiving-antenna, which is often used in experimental set-up for measuring EM field level, could also affect the SE of enclosure. This was numerically demonstrated in [6] and experimentally confirmed in [7].

Several techniques can be applied in order to improve the shielding properties of enclosure over a frequency range. The SE of enclosure was increased by using absorbers [8] or conductive foam in [9] and [10]. As damping techniques, the composite materials based on nanotechnology [11] and metamaterial absorber structure [12] can be used. Furthermore, a frequency-selective surface [14] and polymer composites filled with carbonaceous particles which are suitable for microwave absorption [13] can be employed. The enclosure can be coated with composite foam material or can be made of that material [15]. In [16], it was shown that placing small antenna elements, dipole or loop antenna structure with loaded resistance on the enclosure wall opposite to the enclosure aperture can improve the enclosure SE. The effective length of this small structure was chosen to match the first resonant frequency of enclosure. In papers [17] and [18], the authors proposed to suppress the first resonant frequency in a metal enclosure by putting small antenna elements with loaded resistance. It was shown that the EM shielding could be improved by placing a small dipole printed antenna structure on the enclosure wall inside. The improvement was efficiently, especially at the first resonant frequency over observed frequency range.

In [8], an influence of an electromagnetic interference (EMI) absorber inside the enclosure and its improvement on the enclosure SE was experimentally studied. The absorbers were placed on the back wall of enclosure, on two side walls and on the back and two side walls at the same time. In [1] the study from [8] was expanded placing and combining absorbers on other enclosure walls in order to see how these absorbers positions affect the SE of enclosure, especially at resonant frequencies.

In this paper, the experimental study of absorber sheet position impact on shielding effectiveness of enclosure is systematized and supported by the numerical analysis of the EM field distribution inside inner enclosure walls. For numerical simulations, the TLM method is used aiming to estimate the greatest impact of absorber position inside the enclosure. In such a way, an absorber amount and precisely position can be determined in advance. In experimental and numerical studies, position of thin EMI absorber sheet on one or more inner enclosure walls is considered focusing on SE behavior at the first resonance of enclosure but it is clear that its placement might affect SE at higher resonances as well.

The paper is organized as follows. Section II refers to analytical calculation of enclosure modes. In Section III, the numerical TLM model of enclosure is described. In Section IV, the experimental set-up and measurement procedure are described. Section V presents a physical enclosure's model with the EMI absorber material and with a receiving-antenna inside. Section VI provides discussion of the experimental results. Finally, Section VII summarizes the work.

2. Analytical Calculation of Enclosure Modes

In this section, a rectangular metal enclosure with one aperture on a frontal enclosure wall is described. The enclosure has dimensions of (300 x 300 x 120) mm^3. Symmetrically around the centre on the frontal enclosure wall, a rectangular slot aperture with dimensions of (100 x 5) mm^2 is positioned. The thickness of all enclosure walls is t = 1.5 mm. It is made of copper material.

To start with, the metal enclosure can be analysed as a resonator cavity. A waveguide is a type of a transmission line; a resonator can be constructed from closed sections of waveguide [19]. Since a waveguide is short-circuited at both ends, a closed metal box or cavity is obtained. Inside the cavity, electric and magnetic energy can be stored and power can be dissipated in the metallic walls of the cavity [19]. Usually, coupling to the resonator can be obtained by a small aperture(s) and a small probe or a small loop.

In this paper, an aperture on the frontal enclosure wall is used for coupling to the enclosure while a small probe such as a monopole antenna is employed for measuring the distribution of the EM field inside enclosure.

According to the analytical equation [19], the TE and TM modes which are occurred in considered enclosure are calculated and are given in Table 1.

Table 1 All the resonant modes for TE and TM modes occurred in considered enclosure, in observed frequency range

Resonant frequency mode, $f_{m,n,l}$	GHz
f_{110}	0.707
f_{101}=f_{011}	1.346
f_{111}	1.436
$f_{201} = f_{021}$	1.601
f_{120}=f_{210}	1.118
f_{211}=f_{121}	1.677
f_{220}	1.414
f_{221}	1.887

3. Numerical Model of Enclosure

Before the experimental procedure is conducted, a numerical model of the considered enclosure is designed by using the TLM method as a numerical modelling technique [5]. It is created to resemble to the experimental procedure. The TLM compact wire model is very suitable for modelling an antenna inside enclosure whose purpose is to measure the EM field level and its distribution [6]. This wire model is based on wire segment incorporated into the standard TLM symmetrical condensed node (SCN). The impedances of additional wire network link and short-circuit stub lines depend on the space used and time-step discretization, and also on per-unit length wire capacitance and inductance [20] and [21].

In the numerical model of the enclosure entitled by *D*, a monopole antenna is employed inside. The TLM compact wire model is used to describe the monopole antenna as a wire conductor with a length of l = 60 mm and with a radius of r = 0.1 mm, placed in the middle of the enclosure [6], as shown in Fig. 1. The antenna is also connected to the ground via resistor *R*. A slot aperture on the front wall of enclosure is described by several nodes across each cross-

section dimension. External EM field, represented as a vertically polarized incident plane wave, penetrates into enclosure through aperture and a current induces on the wire. Further, on a resistor *R*, which is loaded at wire base, a voltage generates. This allows measuring numerically the level of EM field inside the enclosure [6] and [18].

Table 2 presents the first three resonant frequencies (the excited TM modes) obtained by using analytical calculation for rectangular resonator (enclosure without aperture/slot) and by using numerical simulations. The first three modes for the enclosure with slot aperture for empty and for enclosure with monopole antenna are obtained by the TLM numerical calculations. The numerical SE results obtained for the empty enclosure and the one with a monopole-receiving antenna are presented in Fig. 2. It can be observed that the first resonant frequency is shifted toward lower frequencies in presence of the monopole antenna inside. The analysis with different antenna radii and different antenna length is given in [6]. The frequency shift can be explained by the perturbation theory, according to that, when a volume ΔV is put inside the resonator, the total interior volume decreases by ΔV, which affects the position of the resonant frequency in that enclosure [19] and [6].

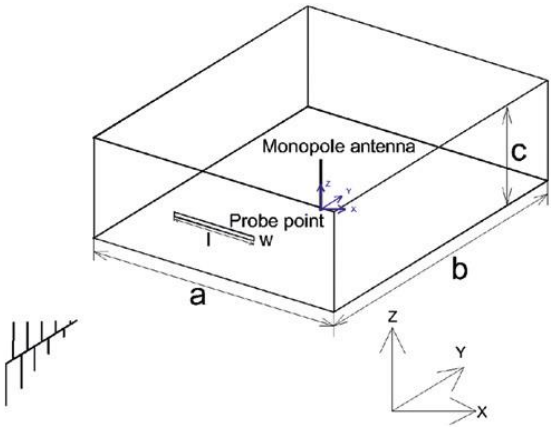

Fig.1 Enclosure *D* with one rectangular aperture on the front wall, excited by normal incident plane wave vertically polarized [6]

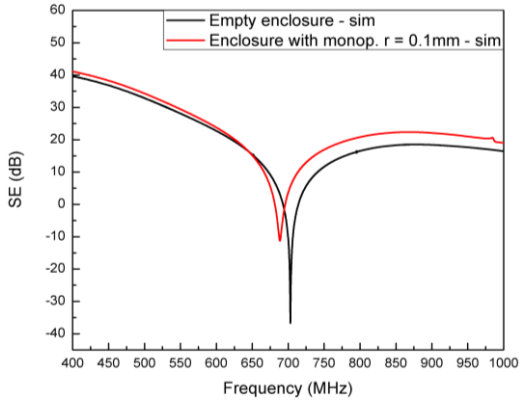

Fig. 2 The first resonant frequency comparative peaks of enclosure *D* with and without monopole antenna (TLM simulations) [6]

Table 2 The first three resonant frequencies in enclosure *D*

TEM mode	Analytical calculation	Empty enclosure [6]	Enclosure with monopole r = 0.1 mm [6]
TM_{110}	f_{110} = 707.107 [MHz]	fr_1 = 703.059 [MHz]	fr_1 = 688.496 [MHz]
TM_{120}	f_{120} = 1118.03 [MHz]	fr_2 = 1101 [MHz]	fr_2 = 1099 [MHz]
TM_{130}	f_{130} = 1581.138 [MHz]	fr_3 = 1608 [MHz]	fr_3 = 1444 [MHz]

4. Experimental Procedure and Setup

The experimental procedure of the equipment under test (EUT) is described in this section. The measurements are conducted in a semi-anechoic room - measuring place occupied with RF absorbers in an ordinary laboratory space, in Laboratory for HF measurements at FERIT Faculty in Osijek, Croatia. In order to determine the SE of enclosure, a measuring procedure has to be performed twice, without and with enclosure. The SE of considered enclosure is measured by the network analyzer and with the s_{21} parameters. The transmission parameters of the measurement without and with an enclosure are marked as s_{21n} and s_{21e}, respectively [8]. The SE can determine by following:

$$SE\ [dB] = s_{21n} - s_{21e}. \tag{2}$$

Figure 3 illustrates the measuring configuration used in a semi-anechoic room. The dipole broadband-antenna, type Vivaldi, was used as a transmitting antenna, in the experimental set-up. The Vector Network Analyzer (VNA), the Keysight Field Fox RF Analyzer N9914A 6.5 GHz, with a maximum power of 3 dBm and with a resolution of 100 Hz was employed as a measuring device. The Vivaldi antenna was connected via coax cable to the VNA. Further, the VNA was connected to the receiving-antenna via coax cable. An in-house monopole antenna was employed as a receiving-antenna and it is placed inside tested *D* enclosure [17] and [18].

In the measurement process, as an excitation source, a vertically polarized Vivaldi antenna is used [21], as depicted in Fig. 3. The Vivaldi antenna has a frequency range of 600 MHz to 6 GHz while a receiving one is a very thin in-house monopole. The monopole antenna is placed in the middle of the enclosure in order to measure the level of EM field inside. All measurements are performed in the frequency range from 600 MHz to 2 GHz, in the far-field.

Enclosure used in experiments is made of copper material with the internal dimensions (300 x 300 x 120) mm^3. An in-house monopole antenna is also made of copper with a length of l = 60 mm and with a radius of r = 0.15 mm. Figure 4 presents a photography of a measuring configuration used for obtaining the experimental results in a semi-anechoic room [21].

The SE results of enclosure with the monopole antenna obtained by the measurements and the numerical simulations are compared and presented in Fig. 5. It can be observed an excellent match between the measurements and the simulation curves.

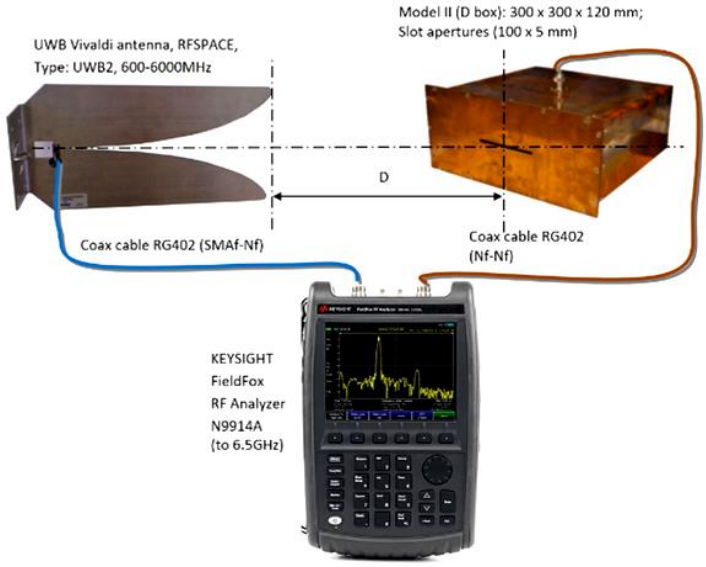

Fig. 3 The sketch of the measuring set-up: transmitting antenna, VNA and EUT (enclosure under test *D*) [21]

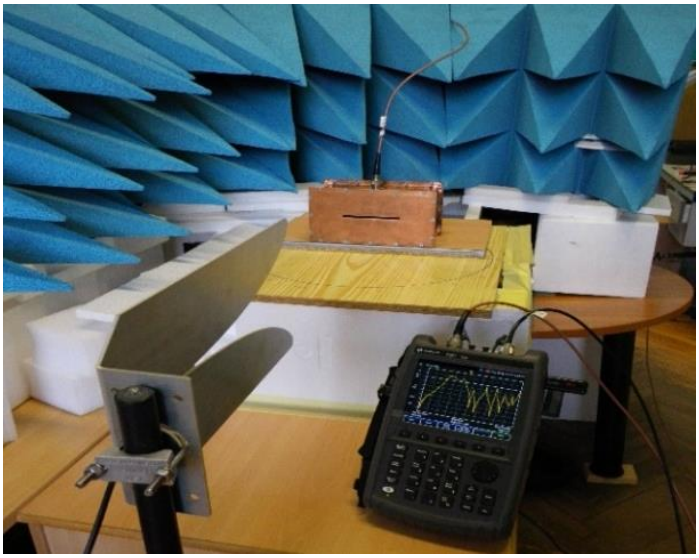

Fig. 4 Photography of measuring configuration used in a semi-anechoic room: transmitting antenna, VNA and EUT (enclosure *D* with a receiving antenna)

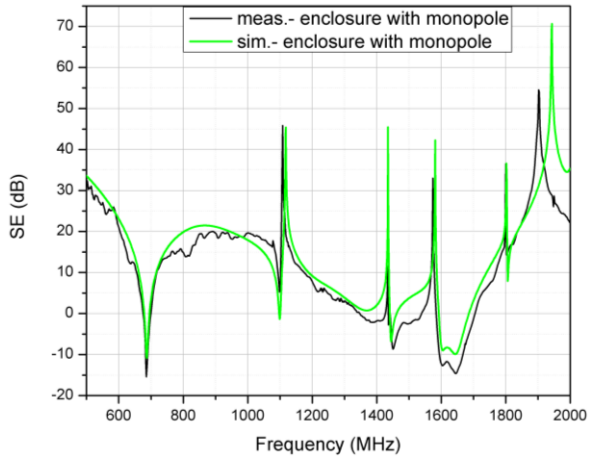

Fig. 5 The comparison between measurements and numerical simulation results of the SE of enclosure with monopole antenna

5. EMI ABSORBER

The 3M™ EMI Absorber AB7050 from AB7000 Series [1], [8] and [22] is used in the measurements conducted in this paper. One side of the absorber sheet consists of a flexible polymer resin loaded with soft metal flakes and on the other side is covered by an acrylic pressure-sensitive adhesive allows for easy application [8] and [22]. This absorber is typically used for applications in the wide frequency range, from 50 Hz up to 10 GHz. It is a broadband EMI absorber designed to work in near-field applications inside and around electronic devices and assemblies [22]. This absorber is thin as a sheet of paper, with the backing thickness of 0.5 mm and adhesive thickness of 0.05 mm, so it does not occupy significant space inside the enclosure [22]. The EMI absorber used in the experimental analysis is cut to fit the inner enclosure's sides.

The experimental procedure is conducted for eight cases (configurations). Firstly, the enclosure without EMI absorber is measured and its SE characteristics is obtained. Secondly, the EMI absorber is employed on the lower wall of enclosure which is entitled by LW. Its dimensions correspond to the inner dimensions of the lower enclosure's wall. The third case refers to the absorbers on two side enclosure's walls (entitled by 2SW). The dimensions of the absorber are cut to fit the enclosure's side walls which is (297 x 120) mm^2. In the fourth case, the absorber on the wall opposite to the front wall with an aperture, so-called back wall (entitled by BcW), is considered. In the fifth case, the absorbers are employed at the same time on lower wall and on two side walls (entitled by LW+2SW, as in Fig. 6). The sixth case, the absorbers are put on lower and back enclosure walls (case LW+BcW). The seventh case, the absorbers are put on lower and upper enclosure's wall (case LW+UP). Finally, the eight case is all above-mentioned absorber positions. This case will be called LW+2SW+BcW+UP.

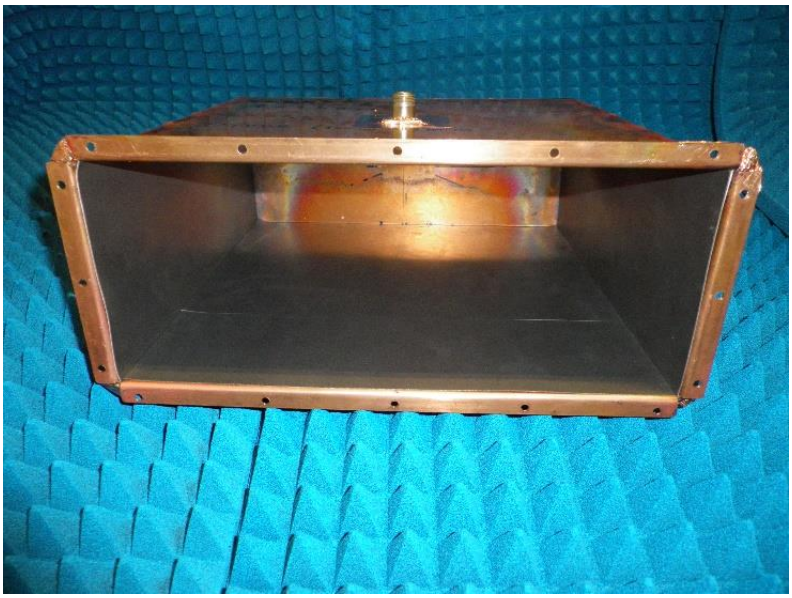

Fig. 6 Photography of the physical model of *D* metal enclosure with the EMI absorbers on lower wall and both side walls of enclosure (LW+2SW)

6. DISCUSSION OF RESULTS

The experimental results of the shielding characteristics of considered enclosure with the EMI absorbers inside are presented in this section. To start with, the SE results are obtained based on the measured transmission parameters without and with the enclosure. In Fig. 7, and also in further figures, the SE results for configuration of the enclosure without absorber (empty enclosure with only receiving antenna inside) are given. The results are compared to the configuration with absorber on the lower enclosure wall and are presented in Fig. 7. It can be observed that the presence of the absorber inside the enclosure gave a significant improvement, especially at the resonant frequencies, over the case without it. Apart from the resonance frequencies, the both SE curves are very similar in terms of the shape and SE levels. Therefore, it can be seen that in the presence of the absorber, all the peaks at resonant frequencies are damped.

Table 3 presents the SE values at the first enclosure resonance for different absorber configurations. Also, it can be seen that the first resonant frequency of empty enclosure occurs at 686 MHz and the SE value is equal to -14.95 dB. A negative SE value might compromise shielding property of the enclosure. By putting the EMI absorber on the lower wall of enclosure, the first resonant frequency occurs at 696 MHz and the positive value of 9.87 dB for the SE is obtained. In comparison between the enclosure with the LW absorber with the one without it, the frequency shift (Δfr_1) of 10 MHz is obtained, as shown in Fig. 7. Moreover, at the first resonant frequency the difference between the SE levels (ΔSE) of 25.32 dB is indicated. Therefore, it can be observed the first resonance frequency shift toward higher frequencies in a presence of the EMI absorber.

Secondly, Fig. 8 presents the compared measurement results of enclosure with the EMI absorbers placed on two side walls to the empty enclosure case. Although the SE curves look similar in Fig. 8 and do not differ much in terms of shape in the whole frequency range, the SE levels are still different at resonant frequencies around 700 MHz, 1100 MHz and 1650 MHz, respectively. It can be seen a very good absorber efficiency at lower frequencies, while it is weaker at higher frequencies in observed range. The additional TE and/or TM modes are not established inside the enclosure, since a very thin EMI absorbers were employed inside it. Also, Table 3 presents that the frequency shift of the first resonance, Δfr_1, is 8 MHz, while the difference between SE levels is 23.65 dB.

For the third case, the absorber is placed on the back wall inside enclosure. The results are depicted in Fig. 9. It can be seen that the difference between the SE levels (ΔSE) is 20.4 dB and the frequency shift (Δfr_1) related to the first resonance position without and with absorber is 8 MHz, as depicted in Fig. 9 and in Table 3.

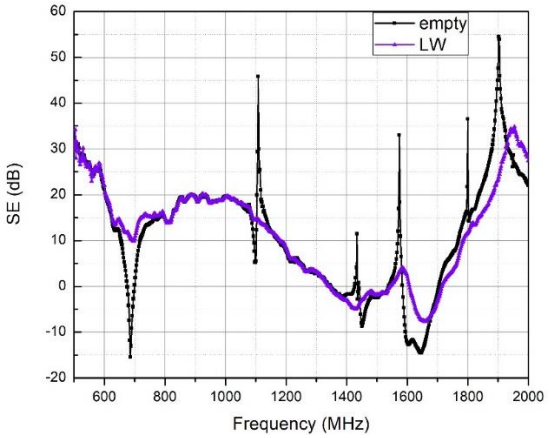

Fig. 7 The SE measurement enclosure results without absorber and with the absorber placed on the lower wall (case LW)

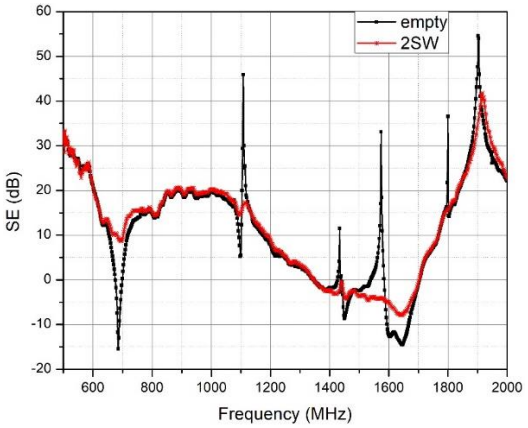

Fig. 8 The measurement results for the SE of the enclosure with the absorber placed on two side walls (case 2SW)

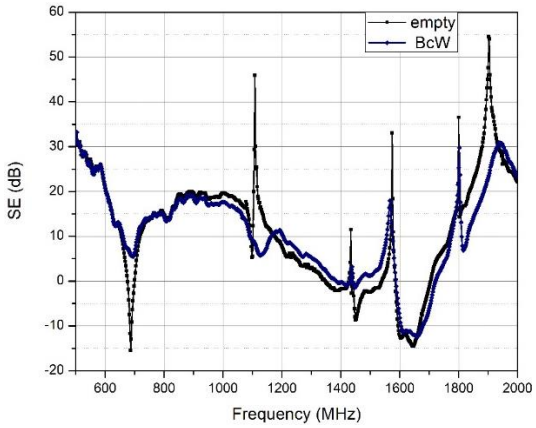

Fig. 9 The measurement results for the SE of the enclosure with the absorber placed on the wall on opposite side from frontal enclosure wall (case BcW)

In order to consider the effects of absorbing material, put in different positions inside the enclosure, on the shielding characteristic, the TLM simulations are conducted. The EM field distribution is shown on different inner wall surface of enclosure without absorber. Figure 10 presents the EM field distribution on the lower wall inside the enclosure. Further, Figs. 11 and 12 present the EM field distribution on the left-side wall and on the back wall inside the enclosure, respectively. It can be observed that the EM field distribution is not uniform and that placing absorber on the lower wall might have the strongest influence on the SE characteristic among these three considered positions. Therefore, position of absorber on the lower enclosure wall is included in all further considered cases.

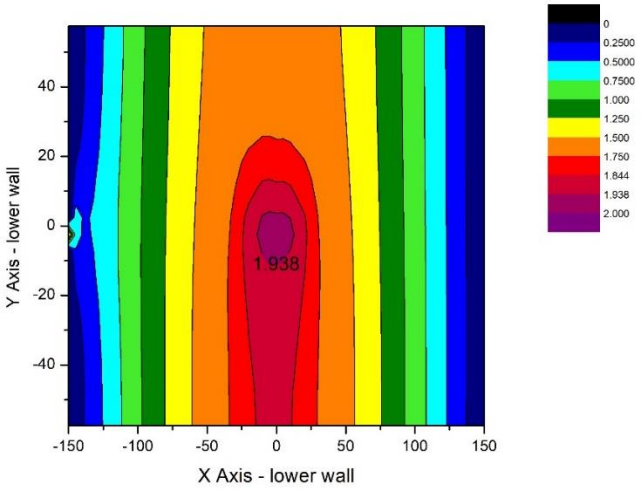

Fig. 10 The EM field distribution on the lower wall inside the enclosure, obtained by the numerical model

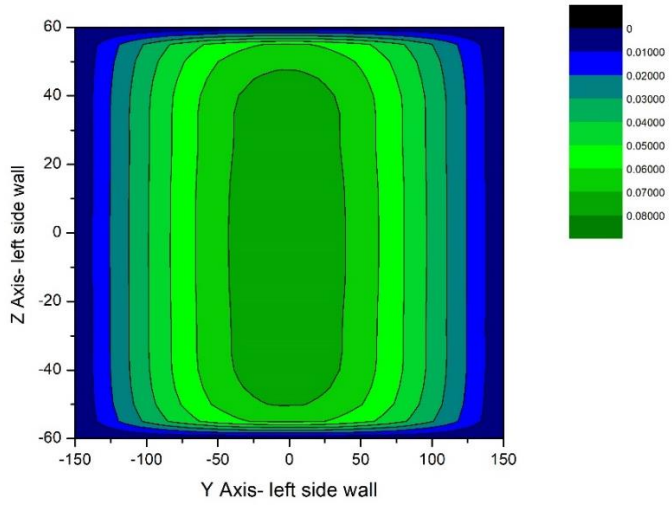

Fig. 11 The EM field distribution on the left-side wall inside the enclosure, obtained by the numerical model

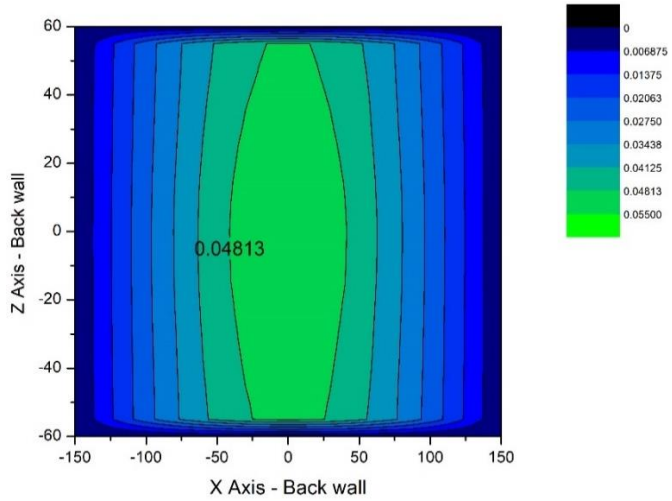

Fig. 12 The EM field distribution on the back wall inside the enclosure, obtained by the numerical model

In Fig. 13, the compared SE measurement results are presented for the first, the fifth, the sixth and the seventh configurations. For the fifth case (LW+2SW), it can be seen that the SE curve do not differ much in terms of shape in the whole frequency range in order to the empty enclosure (the first case), but the SE values differ at resonant frequencies, especially above 1400 MHz. One can notice that the absorber efficiency is very good at lower frequencies, while it is a bit weaker at higher frequencies in observed range. For this configuration, the difference between SE values is 30.54 dB, while the frequency shift Δfr_1 is 10 MHz. The fifth, the sixth

and the seventh configurations have the same frequency shift, see Table 3. Further, for the sixth configuration (LW+BcW) the difference between the SE levels (ΔSE) at the first resonance for this case and the case without the absorbers is 29.2 dB. At higher frequencies, above 1700 MHz, the presence of absorbers for this case led to the decrease of the SE, as depicted in Fig. 13. For the seventh case (LW+UP), the difference between the SE levels (ΔSE) for this case and the case without the absorbers is 28.96 dB, at the first resonance. At higher frequencies, above 1700 MHz, the presence of absorbers influenced to the increase of the SE, for this configuration depicted in Fig. 13. It can be observed that all compared cases have a similar shape of characteristics, but case LW+UP has the highest SE value at the first resonance, as well as significantly higher SE levels at higher frequencies, above 1700 MHz.

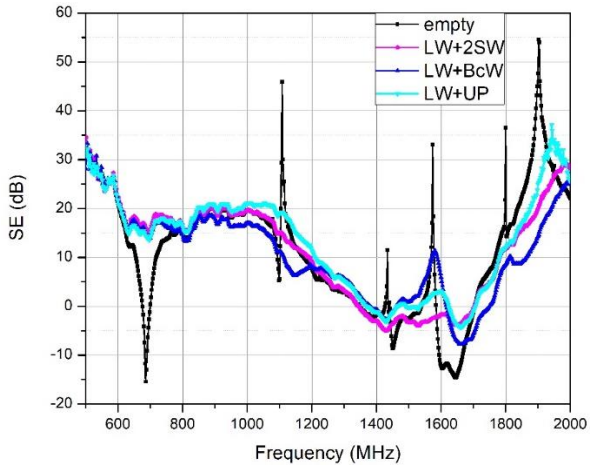

Fig. 13 The comparison of SE measurement results for enclosure without absorber, case LW + 2SW, case LW + BcW and case LW + UP

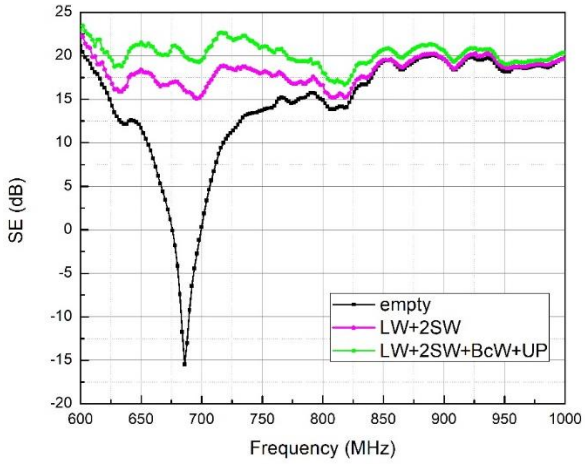

Fig. 14 The comparison of the measured SE of the enclosure around the first resonant frequency – without absorber (empty), case LW+2SW, and case LW+UP+BcW+2SW

Finally, Fig. 14 presents the compared SE characteristics for enclosure without absorber, for the sixth case (LW+2SW) and the configuration where all inner wall surfaces are coated with absorbers, the eight case (LW+UP+BcW+2SW). Obviously, the eight case has a quite better SE level at the first resonant frequency, but bear in mind that it includes a significant amount of absorber materials employed. In practical applications, the case LW+2SW is the most economical one, due to the fact that the significant absorber effects are achieved by using absorber materials only on two walls.

Table 3 The SE values at the first enclosure resonance

EMI Absorber position	fr_1_meas [MHz]	SE_meas [dB]	Δfr_meas [MHz]	ΔSE_meas [dB]
Empty	686	-15.45	-	-
LW	696	9.87	10	25.32
2SW	694	8.70	8	24.15
BcW	694	5.45	8	20.9
LW+2SW	696	15.09	10	30.54
LW+BcW	696	13.75	10	29.2
LW+UP	696	13.51	10	28.96
LW+2SW+BcW+UP	696	19.30	10	34.75

7. CONCLUSION

The eight configurations of the enclosure without absorber and with different positions of absorbers inside are considered in the experimental shielding effectiveness study, supported by numerical analysis. The significant SE level improvement of 30.54 dB at the first resonant frequency, compared to the empty enclosure case, is obtained for the case LW+2SW. The case LW+2SW+BcW+UP gives further improvement of 4.21 dB with respect to case LW+2SW, however, it requires a significantly higher amount of absorber material. Overall, the technique of using thin absorber can improve the shielding properties of enclosure, but to estimate its effects in different positions a numeric study will be beneficial to be carried out. Therefore, a numerical model of EMI absorber will be in future research focus. In addition to that, EMI absorber presence may also influence the SE peaks at the higher frequencies and that will be also further explored.

Acknowledgement: *This work has been supported by the EUROWEB+ project, by the COST IC 1407 and by the Ministry of Education, Science and Technological Development of Republic of Serbia (Grant No. 451-03-68/2022-14/ 200102).*

REFERENCES

[1] N. Nešić, S. Rupčić, V. Mandrić-Radivojević and N. Dončov, "Experimental analysis of a metal enclosure shielding effectiveness improvement with EMI absorber", In Proceedings of the 15th International Online Conference on Applied Electromagnetics - ΠΕС 2021, Niš, 2021, pp. 98–101.

[2] C. Christopoulos, *Principles and Techniques of Electromagnetic Compatibility*, 2nd ed. CRS Press, 2007.

[3] H. A. Mendez, "Shielding theory of enclosures with apertures", *IEEE Trans. Electromagn. Compat.*, vol. 20, no. 2, pp. 296–305, May 1978.

[4] P. M. Robinson, M. T. Benson, C. Christopoulos, F. J. Dawson, D. M. Ganley, C. A. Marvin, J. S. Porter and P. W. Thomas, "Analytical formulation for the shielding effectiveness of enclosures with apertures", *IEEE Trans. Electromagn. Compat.*, vol. 40, no. 3, pp. 240–248, August 1998.
[5] C. Christopoulos, *The Transmission-Line Modelling (TLM) Method*. Piscataway, New Jersey: Wiley-IEEE Press in association with Oxford University Press, May 1995.
[6] N. J. Nešić, and N. Dončov, "Shielding Effectiveness Estimation by using Monopole-receiving Antenna and Comparison with Dipole Antenna", *Frequenz*, vol. 70, no. 5-6, pp. 191–201, April 2016.
[7] N. J. Nešić, Numerical and experimental analysis of aperture arrays impact on the shielding effectiveness of metal enclosures in microwave frequency range, Doctoral thesis, in Serbian, Singidunum University, Belgrade, 2017.
[8] N. J. Nešić, S. Rupčić, V. Mandrić Radivojević and N. Dončov, "Experimental Analysis of Electromagnetic Interferences Absorber Influence on Metal Enclosure Immunity", In Proceedings of the 8th International Conference on Electrical, Electronic and Computing Engineering (IcETRAN). Bosnia and Herzegovina, 2021, pp. 383–386.
[9] X. Luo and D. D. L. Chung, "Electromagnetic interference shielding using continuous carbon-fiber carbon-matrix and polymer-matrix composites", *Elsevier Science, Compos. B Eng.*, vol. 30, no. 3, pp. 227–231, April 1999.
[10] R. Kumar, S. R. Dhakate, P. Saini and R. B. Mathur, "Improved electromagnetic interference shielding effectiveness of light weight carbon foam by ferrocene accumulation", *The Roy. Soc. of Chem. 2013: RSC Advances*, vol. 3, pp. 4145–4151, January 2013.
[11] T. K. Gupta, B. P. Singh, R. B. Mathur and S. R. Dhakate, "Multi-walled carbon nanotube–graphene–polyaniline multiphase nanocomposite with superior electromagnetic shielding effectiveness", *The Royal Society of Chemistry* 2014*: Nanoscale*, vol. 6, p. 842–851, 2014.
[12] F. Costa, S. Genovesi, A. Monorchio and G. Manara, "A Circuit-based Model for the Interpretation of Perfect Metamaterial Absorbers", *IEEE Trans. Antennas and Propag.*, vol. 63, no. 3, pp. 1201–1209, March 2013.
[13] B. A. Munk, *Frequency Selective Surfaces Theory and Design*, New York: John Wiley and Sons, Inc., 2000.
[14] F. Qin and C. Brosseau, "A review and analysis of microwave absorption in polymer composites filled with carbonaceous particles", *J. Appl. Phys.*, vol. 111, p. 061301, March 2012.
[15] A. Ameli, P. U. Jung and C. B. Park, "Electrical properties and electromagnetic interference shielding effectiveness of polypropylene/carbon fiber composite foams", *Elsevier: Carbon*, vol. 60, pp. 379-391, August 2013.
[16] J. Paul, S. Greedy, H. Wakatsuchi and C. Christopoulos, "Measurements and Simulations of Enclosure Damping Using Loaded Antenna Elements", In Proceedings of the IEEE 10th International Symposium on Electromagnetic Compatibility, York, 2011, pp. 676–679.
[17] N. Nešić, B. Milovanović, N. Dončov, V. Mandrić-Radivojević and S. Rupčić, "Improving Shielding Effec-tiveness of a Rectangular Metallic Enclosure with Aperture by Using Printed Dog-bone Dipole Structure", In Proceedings of 52nd International Scientific Conference on Information, Communication and Energy Systems and Technologies (ICEST), Niš, 2017, pp. 97–100.
[18] N. J. Nešić, B. G. Milovanović, N. S. Dončov, S. M. Rupčić and V. Mandrić-Radivojević, "Improving shielding effectiveness of a metallic enclosure at resonant frequencies", In Proceedings of the IEEE 13th International Conference on Advanced Technologies, Systems and Services in Telecommunications (TELSIKS), Niš, 2017, pp. 42–45.
[19] D. M. Pozar, *Microwave Engineering*, 4th ed. Wiley, 2012, Chapters 2-3, pp. 48–162.
[20] V. Trenkić, A. J. Wlodarczyk and R. Scaramuzza, "A Modelling of Coupling between Transient Electromagnetic Field and Complex Wire Structures", *Int. Journal of Num. Modelling*, vol. 12, no. 4, pp. 257–273, July/August 1999.
[21] N. J. Nešić, Slavko S. Rupčić, Nebojša S. Dončov, Vanja Mandrić-Radivojević, "Experimental Shielding Effectiveness Analysis of Metal Plate Influence inside an Enclosure with Aperture", In Proceedings of the IEEE 14th International Conference on Advanced Technologies, Systems and Services in Telecommunications (TELSIKS), Niš, 2019, pp. 190–193.
[22] https://multimedia.3m.com/mws/media/960654O/3m-emi-absorber-ab7000hf-series-halogen-free.pdf